DESY 95–068
April 1995

Dynamical Parton Distributions for α_S Determinations

A. Vogt *

Deutsches Elektronen-Synchrotron DESY
Notkestraße 85, D-22603 Hamburg, Germany

Abstract

Precise determinations of the strong coupling constant in hadronic collisions demand sets of parton densities spanning a sufficiently wide range of values for the QCD scale parameter Λ. For such applications, we supplement the recent GRV parametrization by five sets of dynamically generated parton distributions for Λ-values corresponding to $\alpha_S(M_Z^2)$ between 0.104 and 0.122. Present DIS data, including recent small-x HERA results, do not appreciably discriminate between these sets.

* On leave of absence from Sektion Physik, Universität München, D-80333 Munich, Germany

Parton distributions are essential for connecting observables measured in hard hadronic collisions to the underlying partonic interactions. Parametrizations of these quark and gluon distributions always include a specific value of the QCD scale parameter Λ via the appearance of this quantity in the renormalization group evolution equations. This simple fact leads to a question of consistency [1] when such parametrizations are employed in extractions of the strong coupling constant $\alpha_S(Q^2)$ from data on, e.g., jet production rates at the DESY ep collider HERA [2] or on $W+$jet production at the Fermilab TEVATRON [3]. Hence precise analyses of this type demand sets of parton densities spanning a sufficiently wide range of values for Λ. Recent parametrizations of CTEQ [4], MRS [5, 6] and GRV [7, 8], however, have been provided only for some 'central' values, $\Lambda^{(4)}_{\overline{MS}} = 200 \ldots 250$ MeV, of the NLO ($\overline{\rm MS}$) scale with four active quarks flavours. The only exception is CTEQ2 [4], where one additional large-Λ set has been included.

In this paper, we present five parton density sets which cover, together with the recent GRV parametrization [8], the range of $\Lambda^{(4)}_{\overline{MS}}$ from 150 to 400 MeV in steps of 50 MeV, corresponding to $\alpha_S(M_Z^2)$ between 0.104 and 0.122. For the derivation of these sets we follow the approach developed in [7], in which the quark and gluon densities are generated from valence-like inputs at a very low resolution scale $Q^2 = \mu^2$. Within their uncertainties due to the precise choice of μ^2 [9], those 'dynamical' distributions quantitatively anticipated the strong small-x rise of the proton structure function F_2^p recently observed at HERA [10, 11]. Concerning the present task, it should be noted that this framework provides a close connection between the experimentally tightly constrained quark densities and the much less well-known gluon distribution. This connection leads to parametrizations which are as similar as possible for different values of Λ and thus are very well suited for studying the quantitative importance of the consistency question raised above.

Technically, the present paper closely follows the recent GRV update [8] wherever possible. Our analysis is carried out in the next to leading order (NLO) perturbative QCD framework [12]. We employ the $\overline{\rm MS}$ renormalization and mass factorization schemes with a 'running' number f of active flavours in the QCD beta function and a fixed number of three light partonic quark species present in the Q^2-evolution [13]. The NLO relation connecting $\alpha_S(Q^2)$ and $\Lambda_{\overline{MS}}$ is chosen as in eq. (10) of [8], and the heavy quark thresholds in the beta function are taken to be $Q_h = m_h = 1.5\,(4.5)$ GeV for the charm (bottom) case, respectively. The values of $\Lambda^{(f)}_{\overline{MS}}$, connected by requiring the continuity of α_S at these thresholds, are listed in Table 1 below. The charm contribution to deep inelastic

(DIS) structure functions is approximated by the leading order (LO) massive photon-gluon fusion ('Bethe-Heitler') process [14], since a computationally sufficiently fast version of the next order results of [15], although already announced [16], is not yet available. Here, we use the LO GRV gluon density with $\Lambda^{(4)}_{LO} = 200$ MeV, and the renormalization and factorization scale is fixed at $4m_c^2$, irrespective of the value of Q^2 [13]. For calculating fixed-target and ISR inclusive prompt photon production cross sections the complete NLO program of [17] is utilized, with the photonic fragmentation functions taken from [18]. The small heavy quark contribution to this process is neglected.

The construction of our distributions proceeds in two steps: first we fix the non-singlet quark combinations $u_v \equiv u - \bar{u}$, $d_v \equiv d - \bar{d}$, and $\Delta \equiv \bar{d} - \bar{u}$ by adopting and suitably modifying the corresponding results of a recent global fit [6], then the free parameters of the valence-like sea quark and gluon input densities are determined from data on the proton and deuteron structure functions $F_2^{p,d}$ [19, 20, 21] and on direct photon production in pp collisions [22, 23]. At a reference scale of $Q_0^2 = 4$ GeV^2, the non-singlet densities $f = u_v$, d_v, and Δ are parametrized as

$$xf(x,Q_0^2) = A_f x^{\alpha_f}(1-x)^{\beta_f}(1+\epsilon_f\sqrt{x}+\gamma_f x) \ . \tag{1}$$

For $\Lambda^{(4)}_{\overline{MS}} = 200$ MeV they have been directly adopted from the MRS(A) [6] global fit in [8]. Taking into account that the factorization scheme of [8] slightly differs from the one employed in [6], no readjustment for the small Λ-difference is necessary. For the new sets, corresponding distributions are derived in the following way: the contributions of u_v, d_v, and Δ to F_2 are calculated for $\Lambda^{(4)}_{\overline{MS}} = 200$ MeV in the kinematical region covered by the fixed-target data employed in the MRS(A) analysis, and the new inputs for $\Lambda^{(4)}_{\overline{MS}} \neq 200$ MeV are fitted to these results. For the present purpose, this procedure constitutes a sufficiently accurate substitute for a direct fit to data. The resulting parameters for the input (1) are presented in Table 1.

We now turn to the gluon and sea quark input distributions. Here we first have to fix the low resolution scales $\mu^2(\Lambda)$ at which the valence-like boundary conditions are imposed. In a LO analysis, μ^2, Q^2, and Λ enter the parton density evolution and the DIS structure function F_2 only in the combination $\alpha_S(\mu^2)/\alpha_S(Q^2)$. Therefore, if the quark and gluon densities are forced to be quite similar at a certain 'central' scale Q_1^2 by data, then also the inputs at μ^2 have to be nearly the same irrespective of Λ, provided $\mu^2(\Lambda)$ is chosen by keeping $\alpha_S(\mu^2)/\alpha_S(Q_1^2)$ constant when Λ is changed. In the NLO the situation is slightly complicated by the additional appearance of Λ via $\alpha_S(Q^2)$ in the evolution equations and

$\Lambda^{(4)}$/MeV	150	250	300	350	400
$\Lambda^{(3)}$/MeV	192	301	353	404	453
$\Lambda^{(5)}$/MeV	95	168	206	245	285
$\alpha_S(M_Z)$	0.104	0.113	0.116	0.119	0.122
α_u	0.523	0.547	0.558	0.569	0.581
β_u	3.991	3.926	3.895	3.862	3.829
ϵ_u	-0.30	-0.41	-0.47	-0.51	-0.55
γ_u	5.33	5.03	4.92	4.81	4.68
α_d	0.323	0.332	0.336	0.341	0.345
β_d	4.763	4.664	4.614	4.563	4.510
ϵ_d	4.96	5.25	5.44	5.58	5.81
γ_d	6.06	5.44	5.13	4.78	4.44
A_Δ	0.100	0.0982	0.0974	0.0963	0.0952
α_Δ	0.40	0.40	0.40	0.40	0.40
β_Δ	9.31	9.23	9.18	9.14	9.10
ϵ_Δ	0.0	0.0	0.0	0.0	0.0
γ_Δ	24.5	25.4	25.7	26.2	26.8

Table 1: The NLO ($\overline{\rm MS}$) QCD scales for f active quarks flavours, $\Lambda^{(f)}_{\overline{MS}}$, and the independent non-singlet input parameters for eq. (1). The valence quark normalizations, A_u and A_d, are fixed by the quark number sum rules.

the expressions for F_2. Such effects, however, are already incorporated in the Λ-dependent valence distributions derived above, suggesting that some valence moment should be kept fixed in this case. In fact, adopting the NLO valence quark momentum fraction $< x >_v$ at μ^2 from [8], $< x >_v (\mu^2) = \int_0^1 dx\, x(u_v + d_v)(x, \mu^2) \simeq 0.58$, leads to very similar small-x predictions in the HERA kinematic regime for the different choices of Λ as illustrated in Figure 6 below. The resulting scales $\mu^2(\Lambda)$ are listed in Table 2. Their precise values are, of course, subject to a similar uncertainty [9] as the value for $\Lambda^{(4)}_{\overline{MS}} = 200$ MeV, $\mu^2 = 0.34$ GeV^2 [8].

At these low resolution scales μ^2, the gluon and antiquark distributions are parametrized as

$$\begin{aligned} xg(x,\mu^2) &= A_g x^{\alpha_g}(1-x)^{\beta_g} \\ x(\bar{u}+\bar{d})(x,\mu^2) &= A_\xi x^{\alpha_\xi}(1-x)^{\beta_\xi} \\ xs(x,\mu^2) &= x\bar{s}(x,\mu^2) \,=\, 0 \ . \end{aligned} \tag{2}$$

$\Lambda^{(4)}$/MeV	150	250	300	350	400
μ^2/GeV^2	0.225	0.47	0.62	0.77	0.93
$<x>_v$	0.579	0.582	0.579	0.580	0.582
α_g	1.9	1.9	1.9	1.9	1.9
β_g	4.0	4.0	4.0	4.0	4.0
$2<x>_{\bar{u}+\bar{d}}$	0.140	0.145	0.147	0.150	0.153
α_ξ	0.35	0.33	0.30	0.29	0.27
β_ξ	7.25	6.84	6.62	6.42	6.20

Table 2: The input scales μ^2 and the independent sea and gluon parameters for the valence-like input in eq. (2). The antiquark normalization is expressed via the total sea momentum fraction $2<x>_{\bar{u}+\bar{d}}$, the gluon normalization is fixed by the momentum sum rules.

Our ansatz for the light sea input is slightly simpler than the one in [8], since we do not impose constraints from Drell-Yan lepton pair production in pp interactions on the very small sea quark densities at large x. The resulting difference of the present sets to the NLO GRV parametrization [8] is immaterial, except for very special observables. Due to the energy-momentum sum rule, the ansatz (2) consists of five independent parameters, which are inferred from DIS structure function and direct photon production data. The sea parameters are mainly determined by the $F_2^{p,d}$ results of BCDMS [19] (normalized down by 2.5%), SLAC [20], and NMC [21]. This data is fitted in the region where these structure functions are sensitive to the sea and gluon distributions, $x \leq 0.3$, and where higher-twist contributions are expected to be small, $Q^2 \geq 5$ GeV^2. The large-x gluon density is mainly constrained by the inclusive prompt photon production data of WA70 [22] and R806 [23]. Here, we fix the factorization scale at $\mu_F = 0.5\,p_T$, where p_T denotes the photon transverse momentum, but we allow the renormalization scale μ_R to vary with Λ. It turns out that adopting the gluon shape parameters from the NLO ($\Lambda^{(4)}_{\overline{MS}} = 200$ MeV) analysis of [8] leads to a very good description of the data also for the other Λ-values considered in this paper. We have checked that this agreement can be only marginally improved by fitting α_g and β_g, thus their values are kept fixed. The sea and gluon input parameters for eq. (2) are listed in Table 2.

A detailed comparison of our results to the data used for fixing the valence-like inputs (2) is presented in figs. 1 and 2. We have selected the three sets of distributions derived for $\overline{\Lambda} \equiv \Lambda^{(4)}_{\overline{MS}}\,/\,\mathrm{MeV} = 150$, 250, and 350 for the figures. In fig. 1 we compare our fitted

results with the BCDMS, SLAC, and NMC fixed-target data [19, 20, 21] for F_2^p at $x \leq 0.3$ and $Q^2 \geq 5$ GeV^2, the agreement with the corresponding F_2^d results is very similar. In fig. 2, the pp prompt photon data of WA70 (fixed-target) and R806 (ISR) is compared with our distributions via the 'default quantity', $(\sigma_{exp} - \sigma_{th})/\sigma_{th}$, with σ_{th} given by the $\overline{\Lambda} = 250$ set. All these comparisons exhibit an excellent agreement with the data, irrespective of the value of Λ.

The valence-like gluon and sea input and the valence quark densities at $Q^2 = \mu^2$ are shown in fig. 3. The similarity especially between the quark inputs for different Λ is striking; it should be kept in mind, however, that μ^2 increases by a factor of three when $\Lambda^{(4)}_{\overline{MS}}$ is raised from 150 to 350 MeV. The evolution of these inputs to Q^2 scales of interest for α_S determinations is illustrated in fig. 4 and fig. 5 for the gluon distribution and the quark densities (u and $\bar{u}$), respectively. Finally, fig. 6 shows the dynamical small-x predictions for F_2^p in comparison with recent data from the ZEUS and H1 collaborations [10, 11]. Also shown are the final small-x small-Q^2 results of E665 [24]. Within the present experimental accuracy all sets derived in this paper are in quantitative agreement with the HERA results; the χ^2 for the 149 HERA F_2^p data points lies between 100 and 110, when the systematic and statistical errors are added quadratically and the normalization uncertainties are neglected. Future data may impose substantial constraints, especially at small Q^2, $Q^2 \approx 3$ GeV^2, and very small x where the Λ-effects are most pronounced.

To conclude, we have derived five Λ-variants of the NLO 'dynamical' GRV parton densities, together with the standard set [8] spanning the range from 0.104 to 0.122 for $\alpha_S(M_Z)$, for use in α_S determinations from hadronic collisions. The step size in $\alpha_S(M_Z)$ is about 0.03, which should be sufficiently small for all applications. It remains to be seen whether experimental analyses will soon reach an accuracy that renders the inclusion of Λ-differences in the parton distributions mandatory. The FORTRAN code for calculating these parton densities is available via electronic mail from avogt@x4u2.desy.de.

Acknowledgement

I thank W. Vogelsang for making available the NLO prompt photon production computer code of [17] and for useful discussions.

References

[1] B.R. Webber, Proceedings of the XXVII International Conference on High Energy Physics, Glasgow, July 1994, eds. P.J. Bussey and I.G. Knowles (IOP Publishing, Bristol and Philadelphia, 1995) Vol. I, p. 213

[2] T. Ahmed et al., H1 coll., Phys. Lett. **B346** (1995) 415

[3] J. Kotcher, D0 coll., FERMILAB-CONF-94-323H-E (presented at the 1994 Meeting of the APS, Division of Particles and Fields, Albuquerque 1994)

[4] J. Botts et al., CTEQ coll., Phys. Lett. **B304** (1993) 1993; H.L. Lai et al., CTEQ coll., Michigan State Univ. MSU-HEP-41024 (1994)

[5] A.D. Martin, R.G. Roberts and W.J. Stirling, Phys. Rev. **D47** (1993) 867; Phys. Lett. **B306** (1993) 145; Rutherford Appleton Lab. RAL-95-021 (1995)

[6] A.D. Martin, R.G. Roberts and W.J. Stirling, Phys. Rev. **D50** (1994) 6734

[7] M. Glück, E. Reya and A. Vogt, Z. Phys. **C53** (1992) 127

[8] M. Glück, E. Reya and A. Vogt, DESY 94-206 (1994), Z. Phys. **C**, in press

[9] M. Glück, E. Reya and A. Vogt, Phys. Lett. **B306** (1993) 391

[10] M. Derrick et al., ZEUS coll., Phys. Lett. **B316** (1993) 412; DESY 94-143 (1994)

[11] I. Abt et al., H1 coll., Nucl. Phys. **B407** (1993) 515; T. Ahmed et al., H1 coll., DESY 95-006 (1995)

[12] W. Furmanski and R. Petronzio, Z. Phys. **C11** (1982) 293

[13] M. Glück, E. Reya and M. Stratmann, Nucl. Phys. **B422** (1994) 37

[14] E. Witten, Nucl. Phys. **B104** (1976) 445;
M. Glück and E. Reya, Phys. Lett. **83B** (1979) 98

[15] E. Laenen, S. Riemersma, J. Smith and W.L. van Neerven, Nucl. Phys. **B392** (1993) 162

[16] S. Riemersma, J. Smith and W.L. van Neerven, Phys. Lett. **B347** (1995) 143

[17] L. Gordon and W. Vogelsang, Phys. Rev. **D48** (1993) 3136

[18] M. Glück, E. Reya and A. Vogt, Phys. Rev. **D48** (1993) 116

[19] A.C. Benvenuti et al., BCDMS coll., Phys. Lett. **B223** (1989) 485, ibid. **B237** (1990) 592; A. Milsztain and M. Virchaux, Phys. Lett. **B274** (1992) 221

[20] L.W. Whitlow, Ph.D. Thesis, Stanford University, 1990, SLAC-Report-357 (1990)

[21] P. Amaudruz et al., NMC coll., Phys. Lett. **B295** (1992) 159

[22] M. Bonesini et al., WA70 coll., Z. Phys. **C38** (1988) 37

[23] T. Akesson et al., R806 coll., Sov. J. Nucl. Phys. **51** (1990) 836

[24] A.V. Kotwal, E665 coll., FERMILAB-Conf-95/046-Expt (presented at the XXXth Rencontres de Moriond, QCD and High Energy Interactions, March 1995)

Figure Captions

Fig. 1 The proton structure function F_2^p for our parton density sets with $\overline{\Lambda} \equiv \Lambda^{(4)}_{\overline{MS}}$ / MeV = 150, 250, and 350 compared to the data at medium x and large Q^2 [19, 20, 21] employed in the fit of our sea and gluon inputs (2).

Fig. 2 Comparison of the direct photon production data [22, 23] used for constraining the gluon inputs in (2) with the results of three representative parton density sets. The factorization scale of the calculations is $\mu_F = p_T/2$. Data and curves have been normalized to the $\overline{\Lambda} = 250$ result. $x_T \equiv 2p_T/\sqrt{s}$, where $\sqrt{s}$ is the CMS energy.

Fig. 3 The valence-like input distributions xf ($f = u_v$, d_v, $\bar{u}$, $\bar{d}$, g) at the small scales μ^2 given in Table 2. The strange sea $s = \bar{s}$ vanishes at $Q^2 = \mu^2$.

Fig. 4 The Q^2-evolution of our gluon distributions for $\Lambda^{(4)}_{\overline{MS}} = 150$, 250, and 350 MeV. The results at $Q^2 = 5$ and 10^4 GeV^2 have been multiplied by the numbers indicated.

Fig. 5 The same as Fig. 4, but for the u and $\bar{u}$ quark densities. For clarity, the antiquark distributions are only shown where they substantially differ form the quarks.

Fig. 6 Comparison of our dynamical leading-twist small-x predictions for F_2^p with recent ZEUS [10] and H1 [11] HERA data and low-Q^2 E665 [24] data. Note that these results have not been used in our fits.

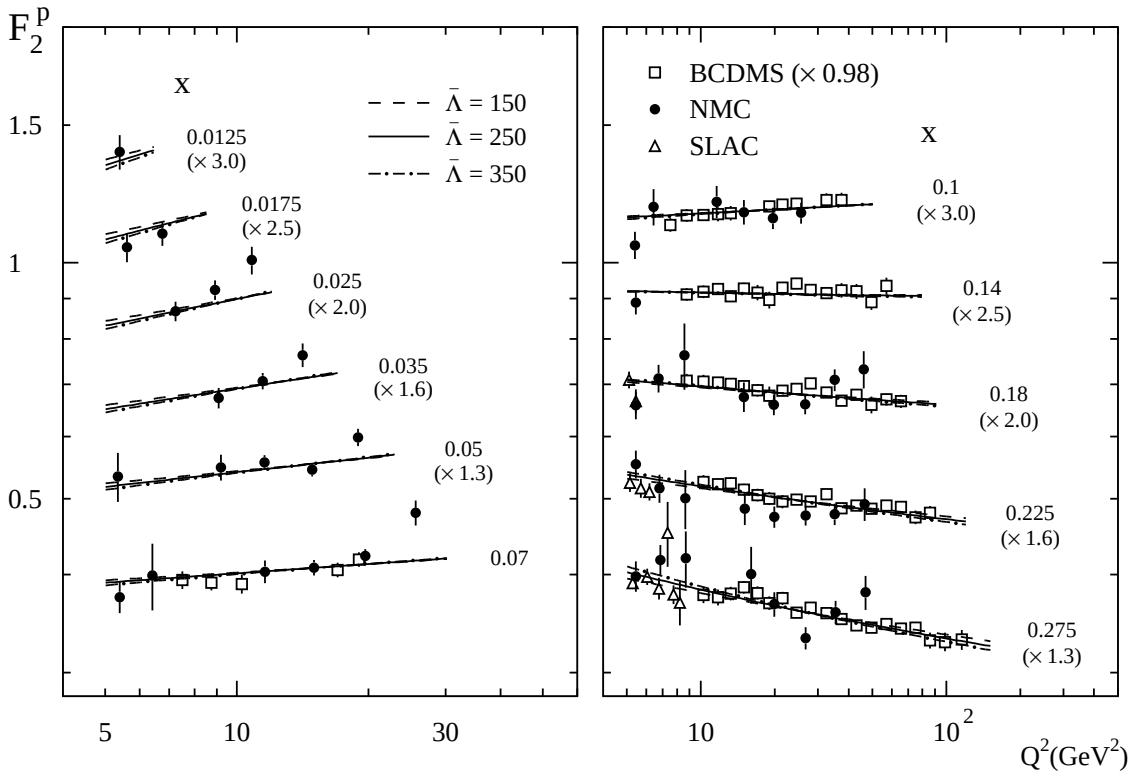
F_2^p
x
$\bar{\Lambda}$ = 150
$\bar{\Lambda}$ = 250
$\bar{\Lambda}$ = 350
0.0125
(× 3.0)
0.0175
(× 2.5)
0.025
(× 2.0)
0.035
(× 1.6)
0.05
(× 1.3)
0.07
1.5
1
0.5
5
10
30
BCDMS (× 0.98)
NMC
SLAC
x
0.1
(× 3.0)
0.14
(× 2.5)
0.18
(× 2.0)
0.225
(× 1.6)
0.275
(× 1.3)
10
10^2
$Q^2(GeV^2)$

Fig. 1

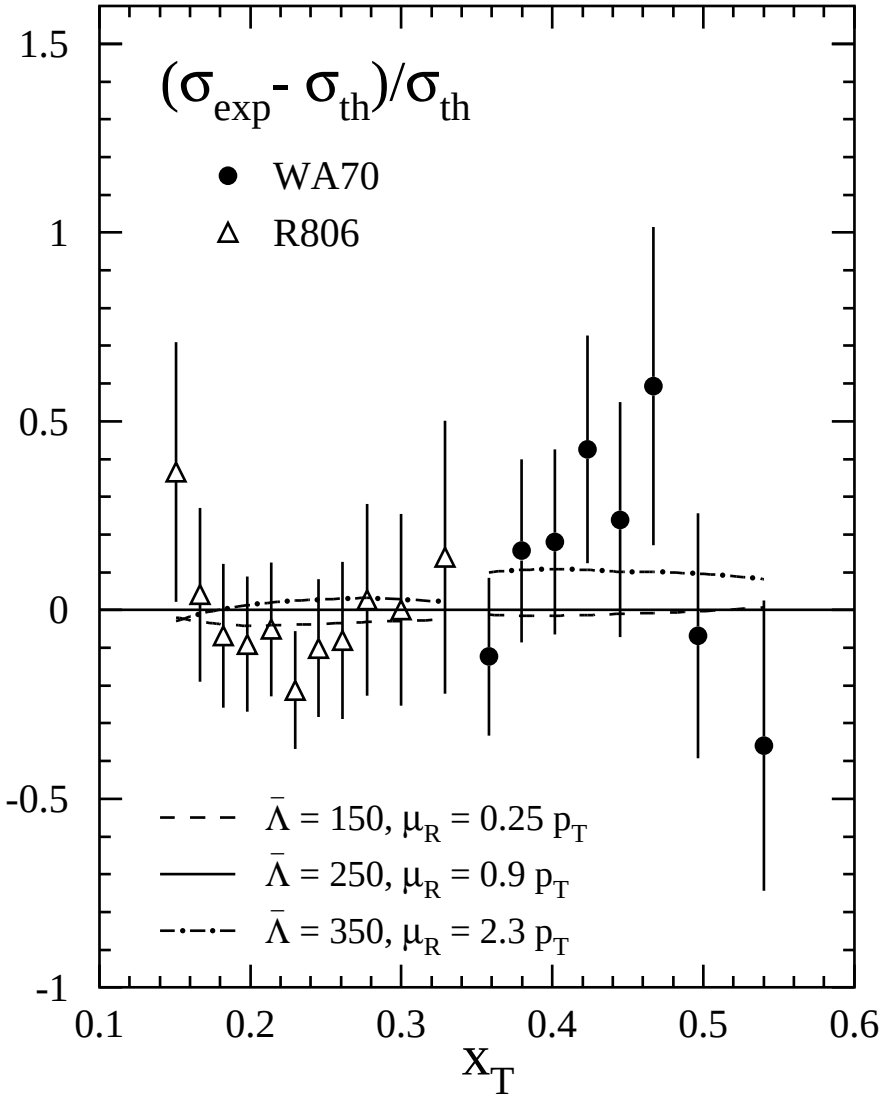
$(\sigma_{exp} - \sigma_{th})/\sigma_{th}$
WA70
R806
$\bar{\Lambda}$ = 150, μ_R = 0.25 p_T
$\bar{\Lambda}$ = 250, μ_R = 0.9 p_T
$\bar{\Lambda}$ = 350, μ_R = 2.3 p_T
1.5
1
0.5
0
-0.5
-1
0.1
0.2
0.3
0.4
0.5
0.6
x_T

Fig. 2

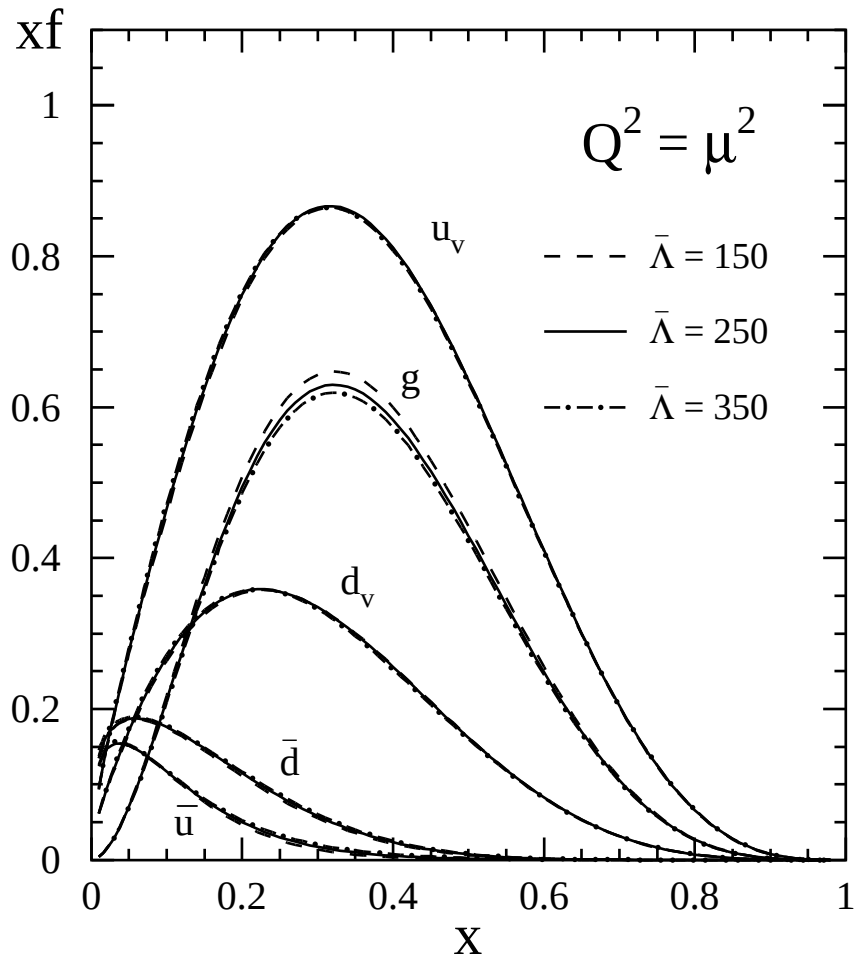
xf
1
0.8
0.6
0.4
0.2
0
0
0.2
0.4
0.6
0.8
1
x
$Q^2 = \mu^2$
u_v
g
d_v
$\bar{d}$
$\bar{u}$
$\bar{\Lambda}$ = 150
$\bar{\Lambda}$ = 250
$\bar{\Lambda}$ = 350

Fig. 3

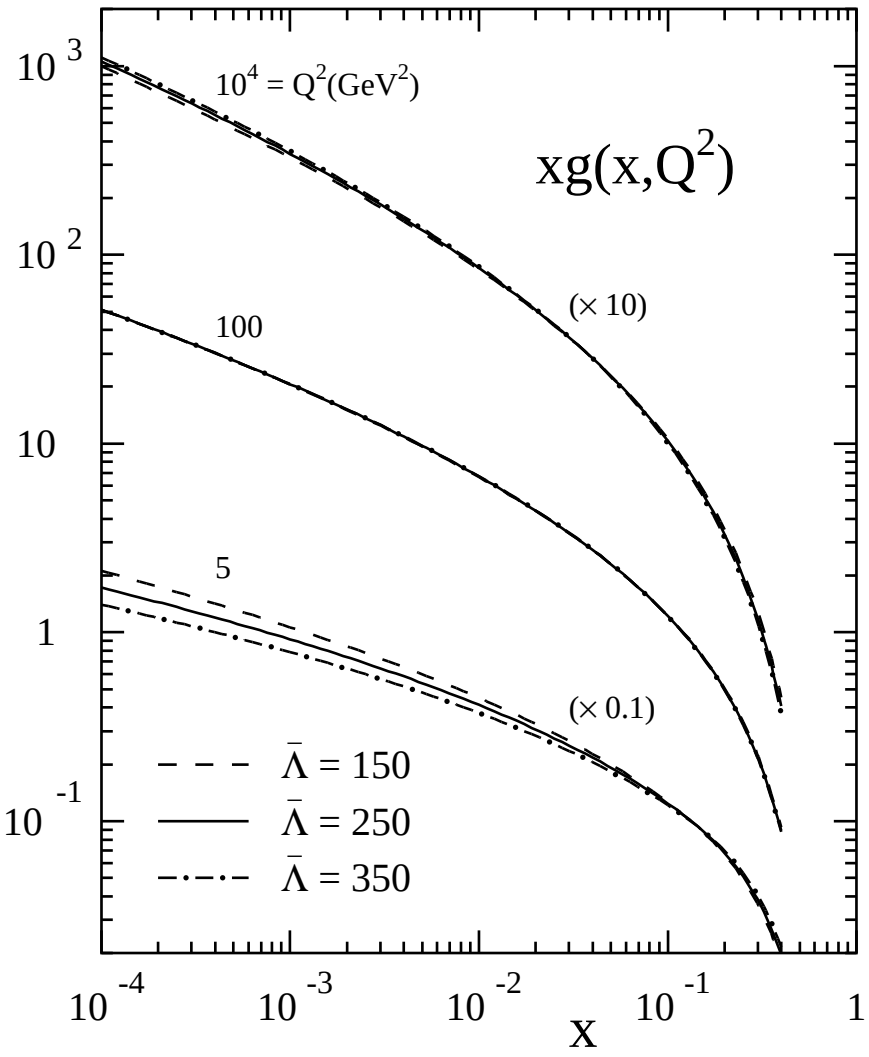
$10^4 = Q^2(GeV^2)$
$xg(x,Q^2)$
(× 10)
100
5
(× 0.1)
$\bar{\Lambda}$ = 150
$\bar{\Lambda}$ = 250
$\bar{\Lambda}$ = 350
10^3
10^2
10
1
10^{-1}
10^{-4}
10^{-3}
10^{-2}
10^{-1}
1
x

Fig. 4

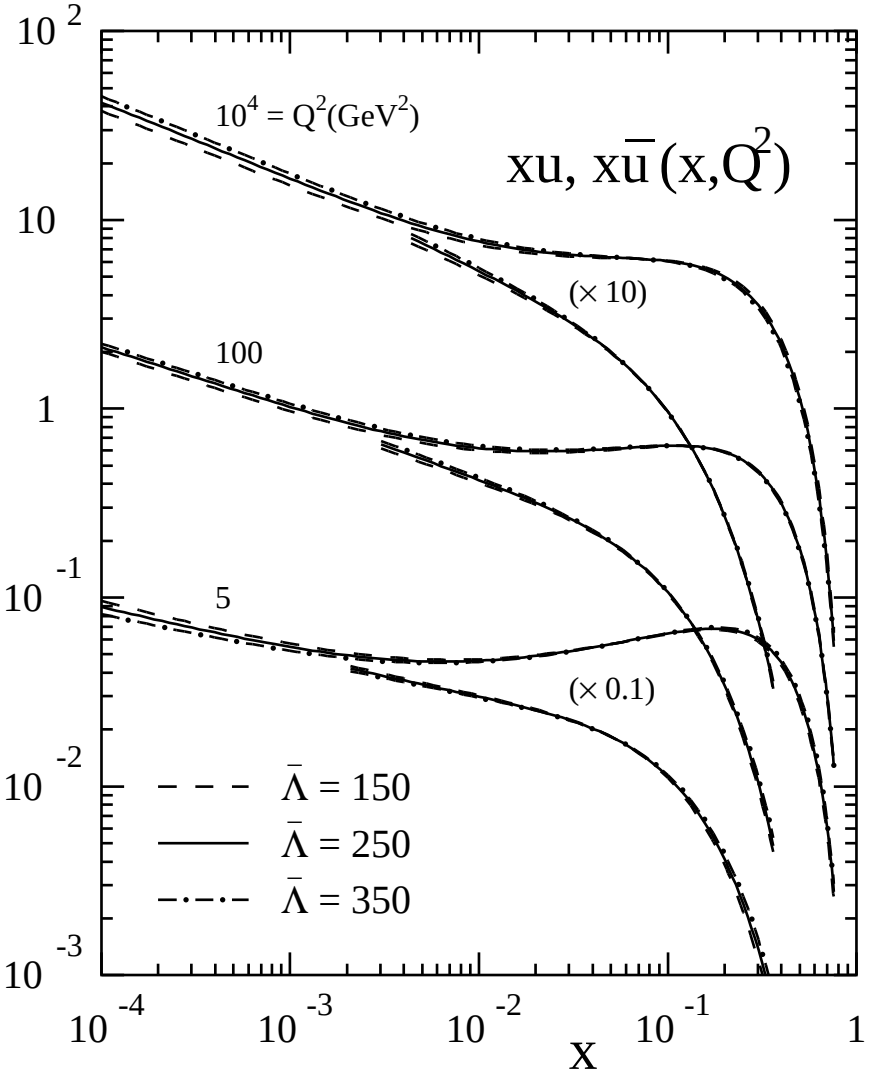
$10^4 = Q^2(GeV^2)$
$xu, x\bar{u}(x,Q^2)$
(× 10)
100
5
(× 0.1)
$\bar{\Lambda}$ = 150
$\bar{\Lambda}$ = 250
$\bar{\Lambda}$ = 350
10^2
10
1
10^{-1}
10^{-2}
10^{-3}
10^{-4}
10^{-3}
10^{-2}
10^{-1}
1
x

Fig. 5

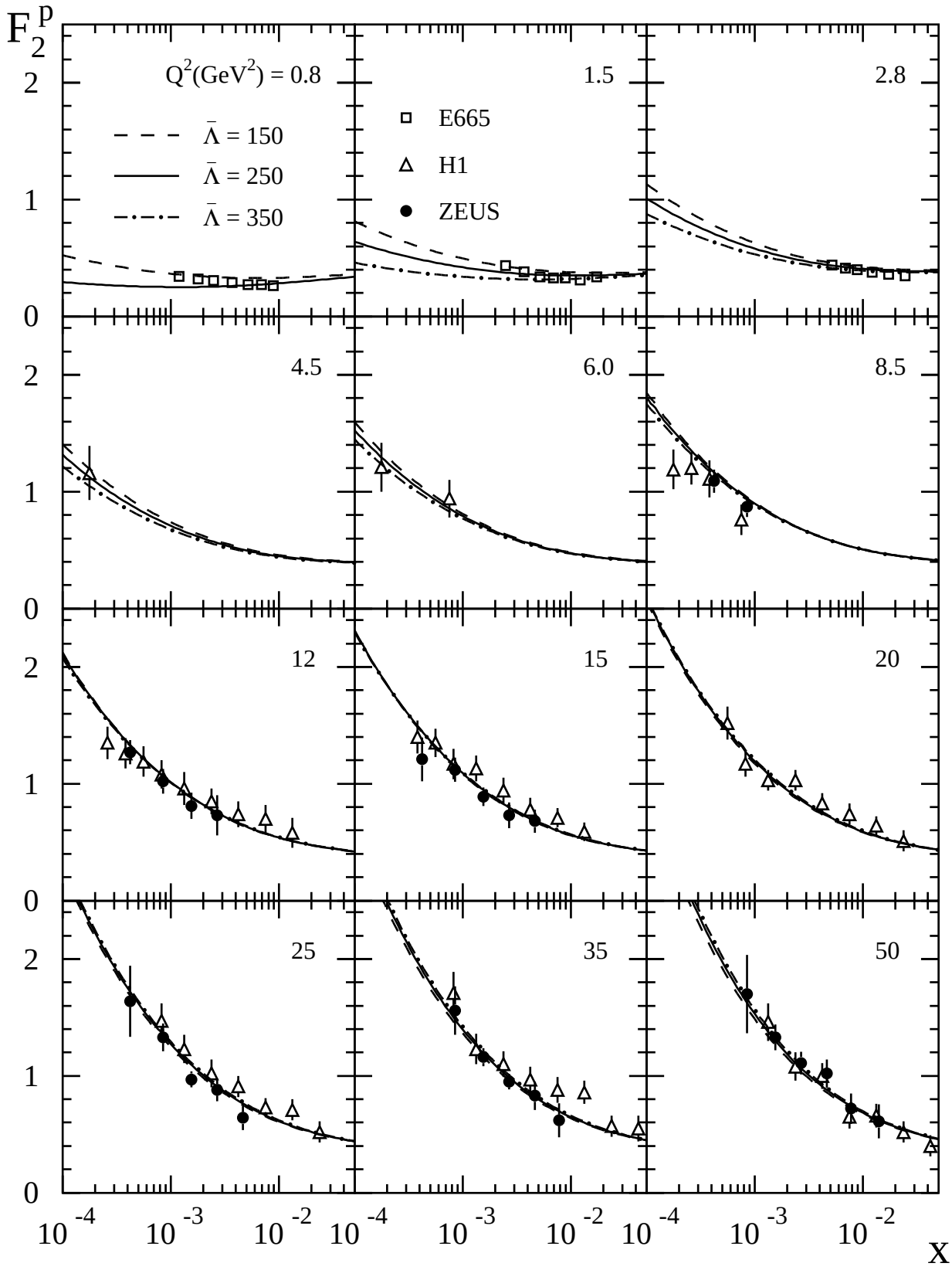
F_2^p
$Q^2(GeV^2) = 0.8$
1.5
2.8
4.5
6.0
8.5
12
15
20
25
35
50
$\bar{\Lambda} = 150$
$\bar{\Lambda} = 250$
$\bar{\Lambda} = 350$
E665
H1
ZEUS
0
1
2
10^{-4}
10^{-3}
10^{-2}
X

Fig. 6